

OXIDATION OF 1,7-OCTADIENE BY MOLECULAR OXYGEN IN LIQUID-PHASE IN THE PRESENCE OF METAL SILICIDES AT THE INITIAL STAGES

Oksana Makota^{1,✉}, Zoryana Komarenska², Lilianna Oliynyk³

¹ Institute of Chemistry and Chemical Technologies, Lviv Polytechnic National University, 12 S. Bandery St., Lviv 79013, Ukraine

✉ oksana.i.makota@lpnu.ua

© Makota O., Komarenska Z., Oliynyk L., 2026

<https://doi.org/10.23939/chcht20.01.072>

Abstract. The effect of metal silicides, TiSi_2 , VSi_2 , MoSi_2 , HfSi_2 , TaSi_2 , and WSi_2 , on the initial stages of the liquid-phase oxidation processes of 1,7-octadiene by molecular oxygen was investigated. It was established that the presence of a homogeneous initiator of radical processes, *tert*-butyl hydroperoxide, was necessary for the oxidation reaction to proceed. VSi_2 is the best catalyst for the oxidation of 1,7-octadiene by O_2 . VSi_2 and MoSi_2 exhibited excellent reusability over five cycles of use without significant loss in their catalytic activity. VSi_2 and MoSi_2 before and after the oxidation reaction were characterized by XRD and FTIR.

Keywords: oxidation, diene, molecular oxygen, hydroperoxide, catalysts, metal silicides.

1. Introduction

The oxidation of hydrocarbons is a key transformation in organic chemistry, leading to the formation of valuable oxygen-containing products such as epoxides, alcohols, ketones, carboxylic acids, and so on.^{1–6} These compounds are essential intermediates in the production of pharmaceuticals, agrochemicals, and polymers.^{7–11} Molecular oxygen is particularly attractive as an oxidant for such reactions due to its natural abundance, low cost, and environmentally friendly nature, as it generates minimal waste and aligns with green chemistry principles. Recent advancements have demonstrated the efficacy of O_2 in various oxidation reactions, highlighting its potential to replace traditional, more hazardous oxidants in both laboratory and industrial settings.^{12–16}

However, direct oxidation of hydrocarbons by molecular oxygen often suffers from low selectivity due to the inert nature of O_2 and its tendency to generate over-

oxidized products. Activating molecular oxygen under mild conditions remains a significant challenge, typically addressed by employing metal-based catalysts.^{17–21} These catalysts play a key role in oxidation reactions by facilitating either radical or non-radical pathways, thereby improving their progress. Furthermore, combining heterogeneous catalysts with radical initiators offers an additional strategy to promote oxygen activation and improve overall reaction performance under mild conditions.

Among metal-based compounds,^{22–31} transition metal silicides^{32–35} have drawn particular attention due to their distinctive characteristics. These intermetallic materials possess unique crystal and electronic structures that set them apart from their constituent metals. They are known for a combination of advantageous physical and chemical properties, including high thermal stability, low electrical resistivity, low work function, and reduced density. These attributes make them highly promising for a variety of technological applications, ranging from nanoelectronics and thermoelectrics to spintronics and field emission devices.

Recently, metal silicides have emerged as a new class of catalytic materials with growing interest in their use for both conventional and advanced chemical transformations.^{32–38} Their well-defined structures contribute to catalytic behaviors that differ substantially from those of traditional metal catalysts. A significant increase in research activity highlights their potential in heterogeneous catalysis, including both classical processes such as oxidation, hydrogenation, dehydrogenation, and methanation, and emerging areas like photocatalysis and electrocatalysis.

In this study, the catalytic ability of metal silicides, TiSi_2 , VSi_2 , MoSi_2 , HfSi_2 , TaSi_2 , and WSi_2 , in the liquid-

phase oxidation processes of 1,7-octadiene by molecular oxygen at the initial stages of the process was investigated.

2. Experimental

2.1. Materials

1,7-Octadiene and chlorobenzene were obtained from Aldrich. The metal silicides (TiSi₂, VSi₂, MoSi₂, HfSi₂, TaSi₂, and WSi₂) were commercial chemicals of chemically pure grade. Molecular oxygen was purified before use. Azodiisobutyronitrile (AIBN) was purified by recrystallization from ethanol. *tert*-Butyl hydroperoxide (TBHP) was synthesized by the procedure given in ³⁹.

2.2. Methods

The oxidation reaction was carried out in a thermostated glass reactor equipped with a temperature-controlled jacket at a temperature of 80 °C, using a volumetric device described in ⁶⁴. The reactor had a diameter of 25 mm and a height of 35 mm. The entire study was performed at the oxygen pressure of 90 kPa under magnetic stirring at 1000 rpm, which ensured a kinetically controlled regime of the process.

The reaction mixture with a volume of 2 mL consisted of diene, chlorobenzene (solvent), and initiators (TBHP or AIBN) in concentrations of [diene]₀ = 5.7 mol/L, [TBHP]₀ = 0.05 mol/L, [AIBN]₀ = 0.05 mol/L. For each experiment, 0.01 g of the metal silicides was loaded into this reaction mixture. The liquid-phase oxidation of 1,7-octadiene was studied at the initial stages of the process, when the influence of the reaction products on the reaction progress could be neglected and avoided.

The initial rate of the oxidation reaction was equal to the initial rate of oxygen consumption, which was determined from the tangent of the slope of the kinetic curve plotted in coordinates of absorbed oxygen volume *versus* reaction time (volume O₂ – time), using the following equation:

$$W_{ox} = \frac{\operatorname{tg}\alpha \cdot P_{O_2} \cdot T_0}{P_0 \cdot V_0 \cdot V \cdot T}$$

where tgα – tangent of the slope of the oxygen absorption kinetic curve in the coordinates volume O₂ – time; P_{O₂} – pressure of oxygen in the system (mm Hg); T₀ – standard temperature (273 K); P₀ – standard pressure (760 mm Hg); V₀ – 22.4 L/mol; V – volume of the oxidation reaction mixture (in our case, it was equal to 2 mL); T – The temperature of the thermostat of the pressure regulator and the gas burette (305 K).

The XRD patterns of VSi₂ and MoSi₂ before and after application in the reaction were recorded on HZG-4 Carl Zeiss diffractometer with a CuKα radiation (λ=0.15406 nm) using a tube voltage of 40 kV and current of 100 mA.

The Fourier transform infrared (FTIR) spectra of VSi₂ and MoSi₂ before and after application in the reaction were recorded on an FTIR 1725×(Perkin-Elmer) spectrophotometer in the range of 500–4000 cm⁻¹ using KBr pellets. The pellet of samples with KBr was formed by compression of the fine powdered mixture under pressure.

3. Results and Discussion

The liquid-phase oxidation of 1,7-octadiene was studied at the initial stages of the process, when the influence of reaction products on the reaction progress could be neglected and avoided. It was found that 1,7-octadiene was not oxidized by molecular oxygen under an oxygen pressure of 90 kPa at a temperature of 80 °C over a reaction time of 2 hours. Moreover, the addition of transition metal silicides to the reaction system did not improve the situation, and no oxidation of 1,7-octadiene occurred under the same conditions within 2 hours. This demonstrated that the liquid-phase oxidation of 1,7-octadiene at the initial stage does not occur in the absence of radical initiators, either with or without metal silicides. Therefore, *tert*-butyl hydroperoxide was used as a homogeneous radical initiator, and the liquid-phase oxidation reaction was carried out under similar conditions.

Kinetic profiles of oxygen consumption in the oxidation of 1,7-octadiene with molecular oxygen in the presence and absence of metal silicide as catalysts, initiated by TBHP as a homogeneous source of radicals, are presented in Figs. 1a,b. It is seen that the introduction of a homogeneous initiator of radical processes, TBHP, in the reaction system favored the reaction proceeding. Oxygen uptaking took place in the oxidation process of 1,7-octadiene with molecular oxygen, applying TBHP both in the presence and in the absence of metal silicides. Moreover, all the investigated transition metal silicides enhance the rate of oxygen consumption compared to the non-catalytic reaction. This indicates the activating effect of metal silicides on the liquid-phase oxidation of 1,7-octadiene with molecular oxygen in the presence of *tert*-butyl hydroperoxide at the initial stages of the process. Fig. 1a shows that the most intense oxygen uptake during the oxidation of 1-octene with molecular oxygen in the presence of TBHP is observed over VSi₂. While in the case of other transition metal silicides, the kinetic curves of molecular oxygen consumption in the oxidation reaction are similar and close to each other (Fig. 1a,b).

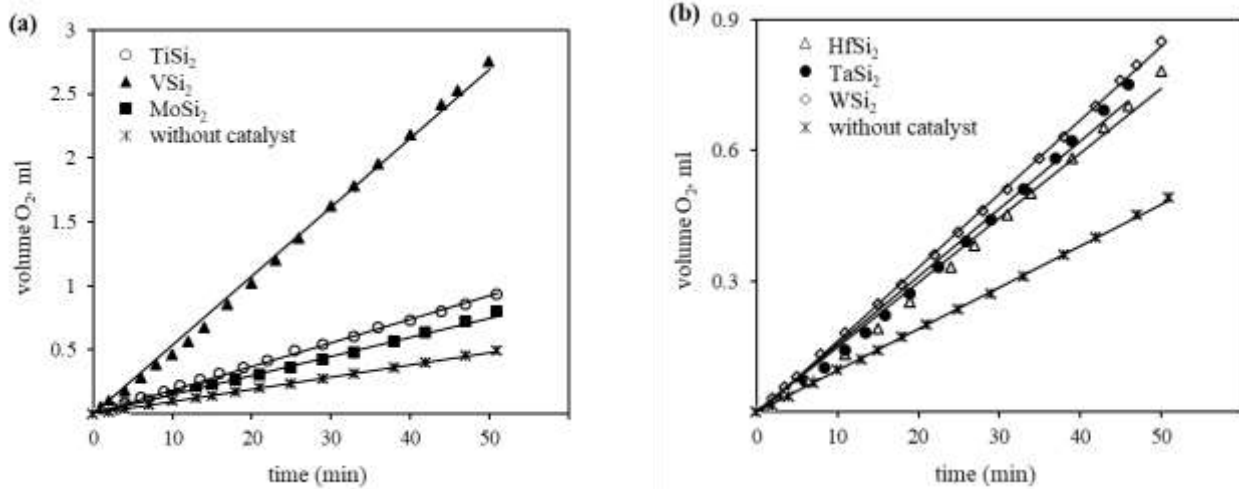


Fig. 1. Kinetic plots of oxygen consumption during the liquid-phase oxidation reaction of 1,7-octadiene by molecular oxygen at the initial stages of the process in the presence of metal silicides: TiSi₂, VSi₂, MoSi₂ (a), and HfSi₂, TaSi₂, WSi₂ (b), and without them (a, b) using *tert*-butyl hydroperoxide as a homogeneous initiator of radical processes

To quantitatively evaluate the catalytic activity of metal silicides, the initial reaction rate of oxidation of 1,7-octadiene by molecular oxygen (W_{ox}) in the presence of *tert*-butyl hydroperoxide at the initial stages of the process was calculated and presented in Fig. 2a. It is seen that the values of oxidation rate of 1,7-octadiene over all metal silicides were higher in 1.6 times for MoSi₂, HfSi₂, TaSi₂,

in 1.7 times for WSi₂, in 1.9 times for TiSi₂, and finally in 5.7 times for VSi₂ than that in their absence. This further confirms that metal silicides can exhibit catalytic activity in this reaction in the presence of TBHP. Meanwhile, vanadium silicide demonstrates the best catalytic performance among them, while the activities of MoSi₂, HfSi₂, and TaSi₂ are the lowest.

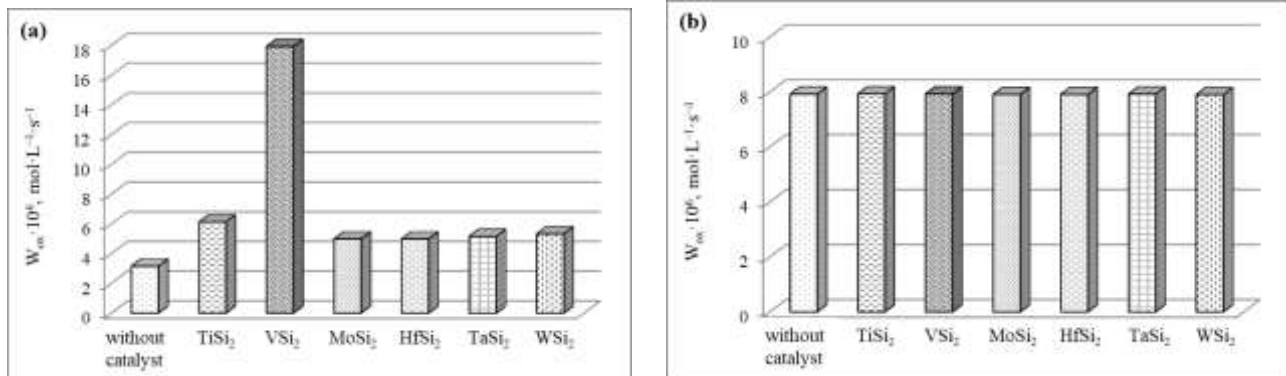
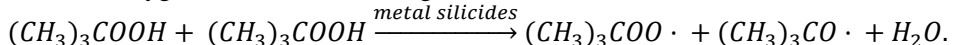


Fig. 2. The initial oxidation rate of 1,7-octadiene by molecular oxygen in the presence and absence of metal silicides using homogeneous initiators of radical processes: *tert*-butyl hydroperoxide (a) or azodiisobutyronitrile (b)

If the investigated transition metal compounds are involved in the chain propagation reaction, such an effect of these compounds on the oxidation reaction should also be observed in the presence of another homogeneous radical initiator, namely, azodiisobutyronitrile (AIBN), as well as in the absence of any initiator, although, as mentioned above, this was not experimentally observed. The rate of the 1,7-octadiene oxidation reaction by

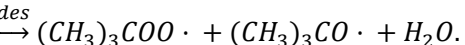
molecular oxygen over metal silicides and without them using AIBN is shown in Fig. 2b. Fig. 2b demonstrates that the oxidation rate for metal silicides remains nearly the same as in their absence in the presence of AIBN in the reaction system. This indicates that metal silicides do not influence the oxidation of 1,7-octadiene in the presence of AIBN, and are not involved in the chain propagation reaction at all.

To summarize, it can be said that the studied metal silicides affect the liquid-phase oxidation of 1,7-octadiene by molecular oxygen at the initial stages



Among the studied metal silicides, the most and least active ones, namely VSi_2 and MoSi_2 , respectively, were selected for further investigation of their stability in the liquid-phase oxidation of 1,7-octadiene by molecular oxygen at the initial stages. The reusability of VSi_2 and MoSi_2 was evaluated over five cycles. This aspect holds particular significance for heterogeneous catalysts due to the feasibility of their recovery and recycling. After completion of each cycle, the catalyst was separated, allowed to dry, and then reintroduced into the following run. The obtained results for VSi_2 and MoSi_2 are shown in Figs. 3a and 3b, respectively. Fig. 3a demonstrates that VSi_2 exhibited excellent stability up to the third cycle and remained moderately stable through the fifth cycle. Its catalytic activity decreased to 99% and 90% of the initial value after the third and fifth reuse, respectively, confirming its potential for practical applications. The catalytic performance of MoSi_2 decreased to 95% and 86% after the third and fifth cycles, respectively (Fig. 3b). These

through the catalysis of the chain initiation reaction, which occurs as a result of the radical decomposition of TBHP:



results indicate good cycling stability of both VSi_2 and MoSi_2 over five cycles.

Moreover, the stability of VSi_2 and MoSi_2 before and after the initial stages of liquid-phase oxidation of 1,7-octadiene by molecular oxygen was also investigated using XRD analysis. Fig. 4 shows the XRD spectra of the initial fresh catalyst, VSi_2 and MoSi_2 , and the catalyst after 1 hour. The diffraction peaks of fresh catalysts corresponding to VSi_2 (JCPDS#65–2645) and MoSi_2 (JCPDS#65–2645) in XRD patterns. No diffraction peaks of SiO_2 can be found in the catalyst samples after application in the oxidation reaction. Furthermore, there is no appearance of oxide products of MoO_3 or V_2O_5 observed in the pattern of already used samples. Thus, according to the XRD pattern, the structure of the catalysts did not change obviously, and only VSi_2 and MoSi_2 were found in the XRD pattern, respectively. The above analysis indicated that VSi_2 and MoSi_2 catalysts were structurally robust after 1 hour of reaction proceeding.

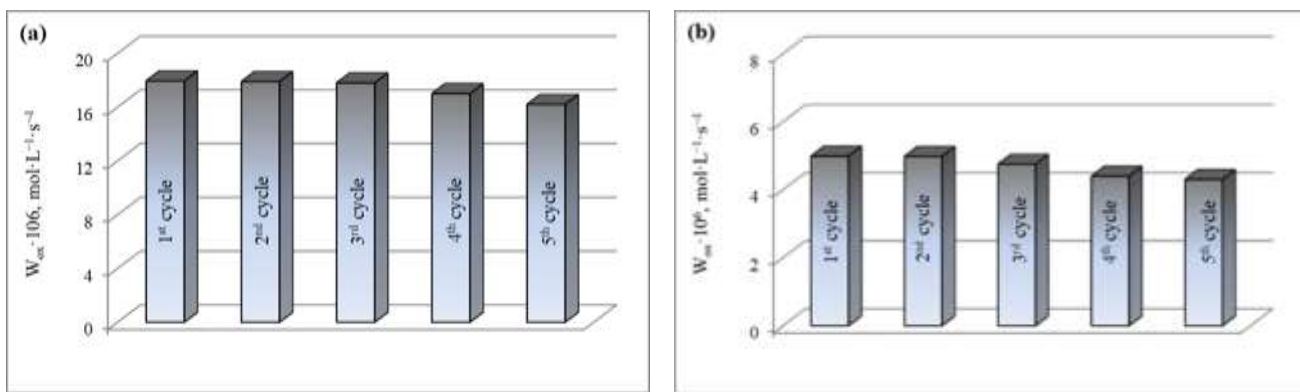


Fig. 3. Reusability of VSi_2 (a) and MoSi_2 (b) during the liquid-phase oxidation reaction of 1,7-octadiene by molecular oxygen at the initial stages of the process

The infrared spectra of VSi_2 and MoSi_2 before and after their application in the liquid-phase oxidation of 1,7-octadiene by molecular oxygen at the initial stages of the process in the range of 500–4000 cm^{-1} are shown in Fig. 5. For better visualization, the narrower range of 850–1500 cm^{-1} is shown in Fig. 6.

Firstly, the initial sample of VSi_2 , as well as the sample after application in the oxidation reaction, contains an intense, wide absorption band centered at 3439 cm^{-1} , which corresponds to the O–H stretching modes of surface-adsorbed molecular water.^{40–42} The band at 1635 cm^{-1} for initial VSi_2 and at 1636 cm^{-1} for VSi_2 after reaction is attributed to the bending mode vibrations of O–H bonds of

adsorbed water.^{40–42} The IR band at 806 cm^{-1} is due to Si–O bending vibrations and is observed in spectra of VSi_2 before and after the reaction.^{40–42} The spectrum of the initial VSi_2 also displays a strong and broad IR band at 1059 cm^{-1} , which can be attributed to the V=O stretching vibrations, which might be covered by the Si–O– asymmetric stretching vibrations.^{40,43,44} A red shift of this signal from 1059 cm^{-1} to 1042 cm^{-1} , along with a decrease in its intensity, is observed in the spectrum of VSi_2 after the oxidation reaction. Another broad band at 1106 cm^{-1} with a shoulder near 1188 cm^{-1} is also observed in the spectrum of the initial VSi_2 , which is usually assigned to the transverse optical (TO) and longitudinal optical (LO) modes of the Si–

O–Si asymmetric stretching vibrations.⁴⁵ While in the spectrum of the used catalyst, an intense absorption band at 1190 cm⁻¹ is observed, which could be assigned to an enhanced shoulder signal of the transverse optical and longitudinal optical modes of the Si–O–Si asymmetric stretching vibrations, presented in the initial catalyst. Additionally, this signal may include contributions from the C–O group,⁴² which newly appear after the reaction and overlap with the blue-shifted signals of the transverse optical and longitudinal optical modes of the Si–O–Si

asymmetric stretching vibrations. Most likely, these bands overlap, or the signal of the C–O group enhances the signal of the Si–O–Si. The formation of this C–O group is most likely due to the adsorption of radical initiator, *tert*-butyl hydroperoxide, on the catalyst surface, which results in the initiation of a radical process. It can also be assumed that the reduced intensity of the band at 1059 cm⁻¹ in the initial sample, along with its shift to 1042 cm⁻¹ in the used sample, may also be attributed to the adsorption of TBHP on the vanadium catalyst.

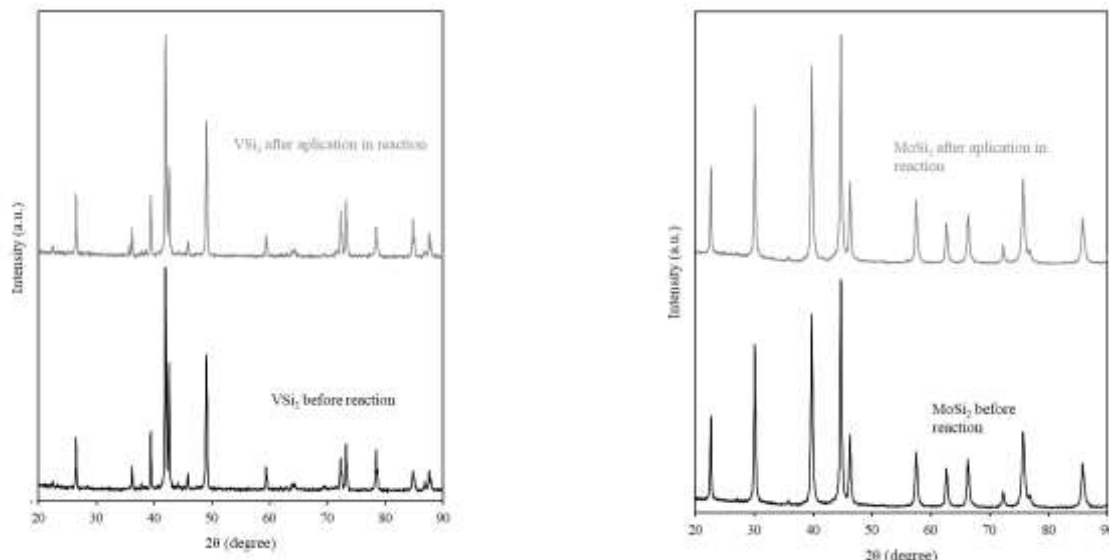


Fig. 4. XRD patterns of VSi₂ and MoSi₂ catalysts before and after the application in the liquid-phase oxidation reaction of 1,7-octadiene by molecular oxygen

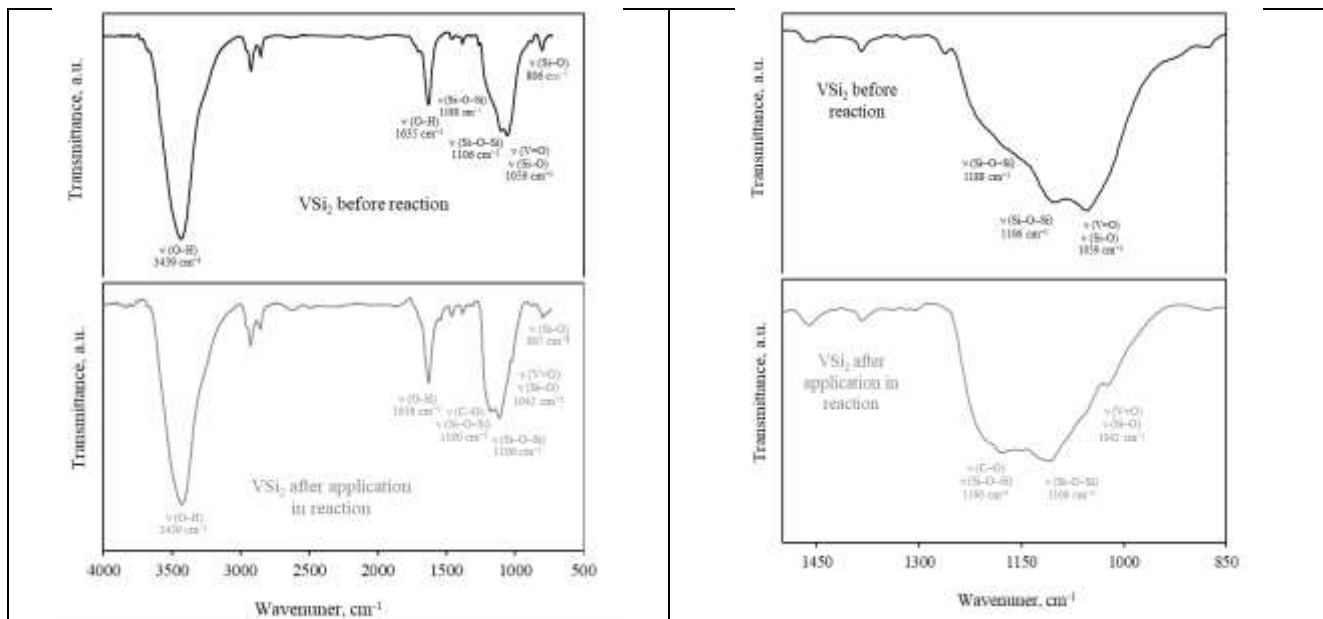


Fig. 5. FTIR spectra of VSi₂ catalyst before and after the application in the liquid-phase oxidation reaction of 1,7-octadiene by molecular oxygen

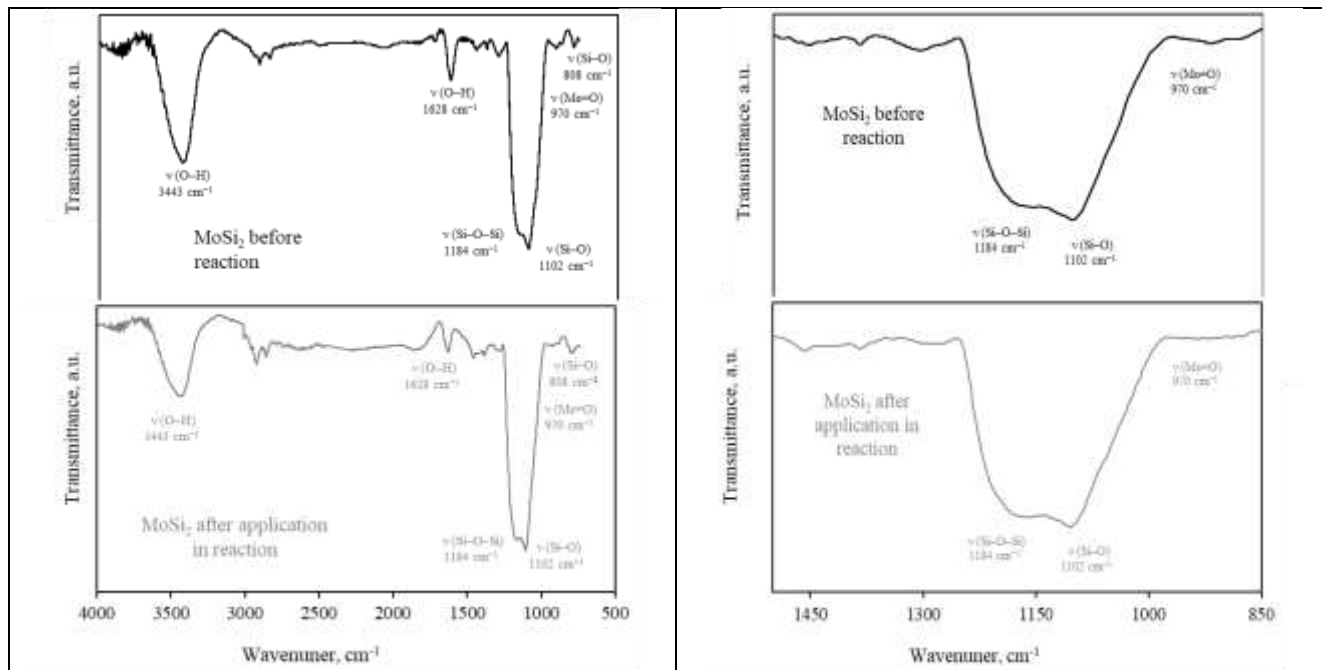


Fig. 6. FTIR spectra of MoSi_2 catalyst before and after the application in the liquid-phase oxidation reaction of 1,7-octadiene by molecular oxygen

The FTIR spectra of MoSi_2 before and after the oxidation reaction remain nearly unchanged. Both initial and used MoSi_2 display bands at 3443 cm^{-1} and 1628 cm^{-1} corresponded to the O–H stretching modes of surface-adsorbed molecular water and the bending mode vibrations of O–H bonds of adsorbed water, respectively.^{40–42} A weak band at 808 cm^{-1} , attributed to Si–O– bending vibrations, is present in both MoSi_2 spectra, as also observed for VSi_2 .^{40–42} The strong broad bands resulting from overlapping peaks at 1184 cm^{-1} and 1102 cm^{-1} are attributed to Si–O–Si and Si–O– asymmetric stretching vibrations, respectively.^{40–42} The signal attributed to the Mo=O stretching vibration, which is expected to appear near 970 cm^{-1} ,⁴⁶ is most likely overlapped by the Si–O– asymmetric stretching vibrations.

Unfortunately, the FTIR spectra of both the initial and used VSi_2 and MoSi_2 samples are dominated by Si–O–Si and Si–O– frameworks vibrations. Additionally, signals corresponding to V=O and Mo=O stretching vibrations are also present in the spectra of VSi_2 and MoSi_2 before and after the reaction. If these signals were observed only in the spectra of the samples after the oxidation reaction, one might assume that the surface of VSi_2 and MoSi_2 oxidation could occur during the oxidation reaction. However, since these signals are found in both the initial and used samples, it can also be assumed that impurities of oxides of these elements are present in the studied samples. However,

since these bands are also present in the spectra of the initial samples and no oxides of these elements were detected by XRD analysis, it is most likely that the surface of the metal silicides can adsorb atmospheric oxygen without actual oxidation. It is in good agreement with results in^{40–42}.

Additionally, noticeable shifts of absorption bands as well as the appearance of the C–O band, most likely as the result of adsorption of radical initiator, are observed only in the case of the most catalytically active VSi_2 , indicating the involvement of the heterogeneous catalyst surface in the process of radical initiation in the oxidation reaction. In contrast, for MoSi_2 , which did not exhibit significant catalytic activity, the FTIR spectra before and after reaction remain nearly the same. It allows us to assume that no significant surface changes of MoSi_2 occurred, and its surface is not involved in the initiation of the process.

4. Conclusions

The catalytic activity of metal silicides, TiSi_2 , VSi_2 , MoSi_2 , HfSi_2 , TaSi_2 , and WSi_2 , in the liquid-phase oxidation processes of 1,7-octadiene by molecular oxygen in the presence of homogeneous initiators of radical processes, namely, *tert*-butyl hydroperoxide and

azodilizobutyronitrile, was studied for the first time. It was established that metal silicides catalyze the oxidation reaction only in the presence of *tert*-butyl hydroperoxide through the catalytic initiation of the chain reaction via the radical decomposition of TBHP, thereby increasing the value of oxidation rate in 1.6 times for MoSi_2 , HfSi_2 , and TaSi_2 ; 1.7 times for WSi_2 ; 1.9 times for TiSi_2 ; and up to 5.7 times for VSi_2 compared to that in their absence. VSi_2 was found to be the most active catalyst among metal silicides, providing an oxidation rate value of nearly $18 \cdot 10^6 \text{ mol} \cdot \text{L}^{-1} \cdot \text{s}^{-1}$.

VSi_2 and MoSi_2 demonstrated good reusability for at least five cycles in the liquid-phase oxidation of 1,7-octadiene by molecular oxygen in the presence of *tert*-butyl hydroperoxide, retaining 99% and 95% of their initial catalytic activity after three cycles, and 90% and 86% after five cycles, respectively. These results confirm the excellent cycling stability and practical potential of both catalysts.

It was shown by XRD results that VSi_2 and MoSi_2 catalysts exhibited excellent structural stability and remained structurally robust after 1 hour of the oxidation reaction. FTIR analysis indicates that the catalytic activity of VSi_2 may be due to the adsorption of *tert*-butyl hydroperoxide on the catalyst surface, followed by radical initiation of the oxidation process.

The application of the most active catalyst, VSi_2 , in the study of the kinetic regularities of the liquid-phase oxidation of 1,7-octadiene by molecular oxygen in the presence of *tert*-butyl hydroperoxide is currently underway and will be reported in a forthcoming publication.

References

[1] Kang, J.; Park, E.D. Liquid-Phase Selective Oxidation of Methane to Methane Oxygenates. *Catalysts* **2024**, *14*, 167. <https://doi.org/10.3390/catal14030167>

[2] Ciriminna, R.; Albanese, L.; Meneguzzo, F.; Pagliaro, M. Hydrogen Peroxide: A Key Chemical for Today's Sustainable Development. *ChemSusChem* **2016**, *9*, 3374–3381. <https://doi.org/10.1002/cssc.201600895>

[3] Kim, M.S.; Yang, G.S.; Park, E.D. Effects of Cu Species on Liquid-Phase Partial Oxidation of Methane with H_2O_2 over Cu-Fe/ZSM-5 Catalysts. *Catalysts* **2022**, *12*, 1224. <https://doi.org/10.3390/catal12101224>

[4] Liu, R.; Wu, H.; Shi, J.; Xu, X.; Zhao, D.; Ng, Y.H.; Zhang, M.; Liu, S.; Ding, H. Recent Progress on Catalysts for Catalytic Oxidation of Volatile Organic Compounds: A Review. *Catal. Sci. Technol.* **2022**, *12*, 6945–6991. <https://doi.org/10.1039/D2CY01181F>

[5] Rizescu, C.; El Fergani, M.; Eftemie, D.-I. Liquid Phase Oxidation of Alkenes and Glycerol with Molecular Oxygen over Mixed-Ligand Copper(II) Complexes Grafted on GO as Catalysts. *Appl. Catal. A Gen.* **2023**, *663*, 119302. <https://doi.org/10.1016/j.apcata.2023.119302>

[6] Denekamp, I.M.; Antens, M.; Slot, T.K.; Rothenberg, G. Selective Catalytic Oxidation of Cyclohexene with Molecular Oxygen: Radical versus Nonradical Pathways. *ChemCatChem* **2018**, *10*, 1035–1041. <https://doi.org/10.1002/cctc.201701538>

[7] Vidal, F.; Smith, S.; Williams, C.K. Ring Opening Copolymerization of Boron-Containing Anhydride with Epoxides as a Controlled Platform to Functional Polyesters. *J. Am. Chem. Soc.* **2023**, *145*, 13888–13900. <https://doi.org/10.1021/jacs.3c03261>

[8] Hanif, M.; Zahoor, A.F.; Saif, M.J.; Nazeer, U.; Ali, K.G.; Parveen, B.; Mansha, A.; Chaudhry, A.R.; Irfan, A. Exploring the Synthetic Potential of Epoxide Ring Opening Reactions toward the Synthesis of Alkaloids and Terpenoids: A Review. *RSC Adv.* **2024**, *14*, 13100–13128. <https://doi.org/10.1039/D4RA01834F>

[9] Printz, G.; Shuvo, R.G.; Schweizer, A.; Ryzhakov, D.; Gourlaouen, C.; Lantigner, L.; Jacques, B.; Messaoudi, S.; Le Bideau, F.; Dagorne, S. N-Heterocyclic Carbene-Initiated Epoxide/Anhydride Ring-Opening Copolymerization: Effective and Selective Organoinitiators for the Production of Various Polyesters. *Polym. Chem.* **2024**, *15*, 3901–3906. <https://doi.org/10.1039/D4PY00778F>

[10] Mitani, R.; Yamamoto, H.; Sumimoto, M. Theoretical Study of the Reaction Mechanism of Phenol–Epoxy Ring-Opening Reaction Using a Latent Hardening Accelerator and a Reactivity Evaluation by Substituents. *Molecules* **2023**, *28*, 694. <https://doi.org/10.3390/molecules28020694>

[11] Kayano, K.; Tsutsumi, T.; Murata, Y.; Ogasa, C.; Watanabe, T.; Sato, R.; Karanjit, S.; Namba, K. Epoxide Ring-Opening Reactions for Abundant Production of Mugineic Acids and Nicotianamine Probes. *Angew. Chem. Int. Ed.* **2024**, *63*, e202401411. <https://doi.org/10.1002/anie.202401411>

[12] Zhao, Y.; Yu, Y.; Li, J.; Xie, J.; He, C. Hydrodechlorination under O_2 Promotes Catalytic Oxidation of CVOCs over Pt/TiO₂ Catalyst at Low Temperature. *Chem. Commun.* **2025**, *61*, 4710–4713. <https://doi.org/10.1039/D4CC06366J>

[13] He, X.; Zhang, Y.; Wang, L.; Li, J.; Liu, Y. Propene Epoxidation with Molecular Oxygen: Advancements from Nanoparticle to Single-Atom Catalysts. *Smart Molecules* **2024**, *3*, 25. <https://doi.org/10.1002/smo.20240025>

[14] Yu, X.; Mao, J.; Wu, B.; Wei, Y.; Sun, Y.; Zhong, L. Boosting Direct Oxidation of Methane with Molecular Oxygen at Low Temperature over Rh/ZSM-5 Catalyst. *ChemCatChem* **2023**, *15*, e202300077. <https://doi.org/10.1002/cctc.202300077>

[15] Yan, L.; Wang, S.; Qian, C.; Zhou, S. Enhancing Oxygen Activation toward Promoted Photocatalytic Oxidation of Methane to Liquid Oxygenates with $\text{ReO}_2@\text{TiO}_2$: The Regulation of Oxygen Affinity. *J. Mater. Chem. A* **2025**, *13*, 4662–4672. <https://doi.org/10.1039/D4TA07559E>

[16] Wang, H.; Xin, W.; Zheng, X.; Zhang, Y.; Li, J.; Wang, X. Mild Oxidation of Methane to Oxygenates with O_2 and CO on Fluorine Modified TS-1 Supported Rh Single-Atom Catalyst in a Flow Reactor. *Catal. Lett.* **2024**, *154*, 259–269. <https://doi.org/10.1007/s10562-023-04298-y>

[17] He, F.; Xu, L.; Wang, H.; Jiang, C. Recent Progress in Molecular Oxygen Activation by Iron-Based Materials: Prospects for Nano-Enabled In Situ Remediation of Organic-Contaminated Sites. *Toxics* **2024**, *12*, 773. <https://doi.org/10.3390/toxics12110773>

[18] Yang, X.; Li, Y.; Zhang, Y.; Wang, Y.; Liu, Y.; Xu, Y.; Zhang, Y.; Wang, X. Controlling Metal-Oxide Reducibility for Efficient C–H Bond Activation in Hydrocarbons. *Angew. Chem. Int. Ed.* **2023**, *62*, e202310062. <https://doi.org/10.1002/anie.202310062>

[19] Wang, Y.; Liu, Y.; Su, Q.; Li, Y.; Deng, L.; Dong, L.; Fu, M.; Liu, S.; Cheng, W. Poly(Ionic Liquid) Materials Tailored by Carboxyl Groups for the Gas Phase-Conversion of Epoxide and CO₂ into Cyclic Carbonates. *J. CO₂ Util.* **2022**, *60*, 101976. <https://doi.org/10.1016/j.jcou.2022.101976>

[20] Doiuchi, Y.; Nakamura, Y.; Kato, M.; Oi, S. Acid-Cooperative Transition Metal-Catalysed Oxygen-Atom-Transfer: Ruthenium-Catalysed C–H Oxygenation. *Adv. Synth. Catal.* **2024**, *366*, 1005–1013. <https://doi.org/10.1002/adsc.202301453>

[21] Etim, U.J.; Bai, P.; Gazit, O.M.; Zhong, Z. Low-Temperature Heterogeneous Oxidation Catalysis and Molecular Oxygen Activation. *Catal. Rev.* **2023**, *65*, 239–425. <https://doi.org/10.1080/01614940.2021.1919044>

[22] Makota, O.; Lisnichuk, M.; Briančin, J.; Bednarcík, J.; Bondarchuk, O.; Melnyk, I. Magnetically Enhanced Fe₃O₄@ZnO and Fe₃O₄@ZnO@Bi₂O_{2.7} Composites for Efficient UV and Visible Light Photodegradation of Methyl Orange and Ofloxacin. *Chemosphere* **2025**, *377*, 144365. <https://doi.org/10.1016/j.chemosphere.2025.144365>

[23] Makota, O.; Dutková, E.; Briančin, J.; Bednarcík, J.; Lisnichuk, M.; Yevchuk, I.; Melnyk, I. Advanced Photodegradation of Azo Dye Methyl Orange Using H₂O₂-Activated Fe₃O₄@SiO₂@ZnO Composite under UV Treatment. *Molecules* **2024**, *29*, 1190. <https://doi.org/10.3390/molecules29061190>

[24] Makota, O.; Yankovych, H. B.; Bondarchuk, O.; Saldan, I.; Melnyk, I. Sphere-Shaped ZnO Photocatalyst Synthesis for Enhanced Degradation of the Quinolone Antibiotic, Ofloxacin, under UV Irradiation. *Environ. Sci. Pollut. Res.* **2024**, *31*, 33619. <https://doi.org/10.1007/s11356-024-33619-w>

[25] Komarenska, Z.; Oliynyk, L.; Makota, O. Activation of Mo₂B Catalyst in the Epoxidation Reaction of α -Ethylallyl Ethyl Acrylate with tert-Butyl Hydroperoxide. *Chem. Chem. Technol.* **2023**, *17*, 18–23. <https://doi.org/10.23939/chcht17.01.018>

[26] Ischenko, O. V.; Dyachenko, A. G.; Saldan, I.; Lisnyak, V. V.; Diyuk, V. E.; Vakaliuk, A. V.; Yatsymyrskyi, A. V.; Gaidai, S. V.; Zakharova, T. M.; Makota, O.; *et al.* Methanation of CO₂ on Bulk Co–Fe Catalysts. *Int. J. Hydrogen Energy* **2021**, *46*, 37860–37871. <https://doi.org/10.1016/j.ijhydene.2021.09.034>

[27] Khalameida, S.; Samsonenko, M.; Sydorchuk, V.; Zakutevskyy, O.; Starchevskyy, V.; Lakhnik, A. Improving the Photocatalytic Properties of Tin Dioxide Doped with Titanium and Copper in the Degradation of Rhodamine B and Safranin T. *React. Kinet. Mech. Catal.* **2022**, *135*, 1665–1685. <https://doi.org/10.1007/s11144-022-02206-w>

[28] Starchevskyy, V.; Shparij, M.; Hryncuk, Y.; Reutskyy, V.; Kurta, S.; Hatsevych, O. Modification of the Catalytic System for the Industrial Chlorine Processing of Ethylene in 1,2-Dichloroethane. *Chem. Chem. Technol.* **2020**, *14*, 394–402. <https://doi.org/10.23939/chcht14.03.394>

[29] Shparij, M.; Starchevskyy, V.; Znak, Z.; Mnykh, R.; Poliuzhyn, I. Extraction of Iron-Containing Catalyst from Chlororganic Wastes Generated by Ethylene Chlorination. *East.-Eur. J. Enterp. Technol.* **2020**, *2*(10(104)), 19–26. <https://doi.org/10.15587/1729-4061.2020.201696>

[30] Khalameida, S.V.; Samsonenko, M.N.; Sydorchuk, V.V.; Starchevskyy, V.L.; Zakutevskyy, O.I.; Khyzhun, O.Yu. Photocatalytic Properties of Tin Dioxide Doped with Chromium(III), Silver and Zinc Compounds in the Oxidation of Organic Substrates by the Action of Visible Light. *Theor. Exp. Chem.* **2017**, *53*, 40–46. <https://doi.org/10.1007/s11237-017-9499-5>

[31] Nikipanchuk, M.V.; Komarenskaya, Z.M.; Cherniy, M.O. On the Activation of Mo₂B and MoB Catalysts in Oct-1-ene Epoxidation with *tert*-Butyl Hydroperoxide. *Kinet. Catal.* **2014**, *55*, 212–216. <https://doi.org/10.1134/S0023158414020062>

[32] Ahmad, I.; Aftab, M. A.; Fatima, A.; Mekkey, S. D.; Melhi, S.; Ikram, S. A Comprehensive Review on the Advancement of Transition Metals Incorporated on Functional Magnetic Nanocomposites for the Catalytic Reduction and Photocatalytic Degradation of Organic Pollutants. *Coord. Chem. Rev.* **2024**, *514*, 215904. <https://doi.org/10.1016/j.ccr.2024.215904>

[33] Chen, X.; Liang, C. Transition Metal Silicides: Fundamentals, Preparation and Catalytic Applications. *Catal. Sci. Technol.* **2019**, *9*, 4785–4820. <https://doi.org/10.1039/C9CY00533A>

[34] Yang, K.; Chen, X.; Wang, L.; Zhang, L.; Jin, S.; Liang, C. SBA-15-Supported Metal Silicides Prepared by Chemical Vapor Deposition as Efficient Catalysts Towards the Semihydrogenation of Phenylacetylene. *ChemCatChem* **2017**, *9*, 348–355. <https://doi.org/10.1002/cctc.201601653>

[35] Su, Y.; Xie, Y.; Qin, H.; Huang, Z.; Yin, Q.; Li, Z.; Zhang, R.; Zhao, Z.; Wu, F.; Ou, G. Ultrafine Molybdenum Silicide Nanoparticles as Efficient Hydrogen Evolution Electrocatalyst in Acidic Medium. *Int. J. Hydrogen Energy* **2022**, *47*, 28924–28931. <https://doi.org/10.1016/j.ijhydene.2022.06.218>

[36] Yang, X.; Wan, Y.; Li, J.; Liu, J.; Wang, M.; Tao, X. High Emissivity MoSi₂–SiC–Al₂O₃ Coating on Rigid Insulation Tiles with Enhanced Thermal Protection Performance. *Materials* **2024**, *17*, 220. <https://doi.org/10.3390/ma17010220>

[37] Trach, Y. B. Specifics of Oxidation of Octene-1 with Molecular Oxygen on Vanadium Disilicide. *Petrol. Chem.* **2009**, *49*, 393–396. <https://doi.org/10.1134/S0965544109050107>

[38] Makota, O.I.; Trach, Y.B. Catalysis of 1-Octene Hydroperoxide Epoxidation Reaction by Metal Disilicides. *Pol. J. Chem.* **2008**, *82*, 345–352.

[39] Milas, N.A.; Surgenor, D.M. Studies in Organic Peroxides. VIII. t-Butyl Hydroperoxide and Di-t-butyl Peroxide. *J. Am. Chem. Soc.* **1946**, *68*, 205–208. <https://doi.org/10.1021/ja01206a017>

[40] Liang, Y.; Ouyang, J.; Wang, H.; Wang, W.; Chui, P.; Sun, K. Synthesis and Characterization of Core–Shell Structured SiO₂@YVO₄:Yb³⁺,Er³⁺ Microspheres. *Appl. Surf. Sci.* **2012**, *258*, 3689–3694. <https://doi.org/10.1016/j.apsusc.2011.12.006>

[41] Trach, Y.; Makota, O.; Skubiszewska-Zięba, J.; Borowiecki, T.; Leboda, R. FTIR Investigation into Transition Metal Disilicides as Catalysts for *tert*-Butyl Hydroperoxide Decomposition. *Transit. Met. Chem.* **2010**, *35*, 345–348. <https://doi.org/10.1007/s11243-010-9333-6>

[42] Makota, O.; Trach, Y.; Leboda, R.; Skubiszewska-Zięba, J. The Study of Cyclooctene Oxidation with Molecular Oxygen Catalyzed by VS₂. *Cent. Eur. J. Chem.* **2009**, *7*, 731–738. <https://doi.org/10.2478/s11532-009-0096-x>

[43] Shafeeq, K.M.; Athira, V.P.; Raj Kishor, C.H.; Aneesh, P.M. Structural and Optical Properties of V₂O₅ Nanostructures Grown by Thermal Decomposition Technique. *Appl. Phys. A* **2020**, *126*, 586. <https://doi.org/10.1007/s00339-020-03770-5>

[44] Wen, A.; Cai, Z.; Zhang, Y.; Liu, H. A Novel Method of Preparing Vanadium-Based Precursors and Their Enhancement Mechanism in Vanadium Nitride Preparation. *RSC Adv.* **2022**, *12*, 13093–13101. <https://doi.org/10.1039/d2ra00584k>

[45] Musić, S.; Filipović-Vinceković, N.; Sekovanić, L. Precipitation of Amorphous SiO₂ Particles and Their Properties. *Braz. J. Chem. Eng.* **2011**, *28*, 89–94. <https://doi.org/10.1590/S0104-66322011000100011>

[46] Jun, S.E.; Choi, S.; Choi, S.; Lee, T. H.; Kim, C.; Yang, J. W.; Choe, W.-O.; Im, I.-H.; Kim, C.-J.; Jang, H.W. Direct Synthesis of Molybdenum Phosphide Nanorods on Silicon Using Graphene at the Heterointerface for Efficient

Photoelectrochemical Water Reduction. *Nano-Micro Lett.* **2021**, *13*, 81. <https://doi.org/10.1007/s40820-021-00605-7>

Received: June 01, 2025 / Revised: July 22, 2025 / Accepted: September 05, 2025

**ОКИСНЕННЯ 1,7-ОКТАДІСНУ
МОЛЕКУЛЯРНИМ КИСНЕМ
У РІДИННІЙ ФАЗІ У ПРИСУТНОСТІ СИЛІЦІДІВ
МЕТАЛІВ НА ПОЧАТКОВИХ СТАДІЯХ**

Анотація. Досліджено вплив силіцидів металів, TiSi₂, VSi₂, MoSi₂, HfSi₂, TaSi₂ та WSi₂, на початкові стадії процесу рідиннофазного окиснення 1,7-октадісну молекулярним киснем. Встановлено, що наявність гомогенного ініціатора радикальних процесів — трет-бутилгідропероксиду — є необхідною умовою для перебігу реакції окиснення. VSi₂ є найкращим каталізатором для окиснення 1,7-октадісну. VSi₂ і MoSi₂ проявляють відмінну стабільність при багаторазовому використанні протягом п'яти циклів без істотної втрати каталізаторної активності. VSi₂ і MoSi₂ до та після реакції окиснення були охарактеризовані методами рентгенівської дифракції й інфрачервоної спектроскопії.

Ключові слова: окиснення, дісн, молекулярний кисень, гідропероксид, каталізатори, силіциди металів.